Prostate Cancer: PET with ^{18}F-FDG, ^{18}F- or ^{11}C-Acetate, and ^{18}F- or ^{11}C-Choline

Hossein Jadvar

Department of Radiology, Keck School of Medicine, University of Southern California, Los Angeles, California

Learning Objectives: On successful completion of this activity, participants should be able to describe (1) the potential role of imaging in prostate cancer and (2) the current evidence on the use of ^{18}F-FDG, ^{18}F- or ^{11}C-acetate, and ^{18}F- or ^{11}C-choline in the imaging evaluation of prostate cancer.

Financial Disclosure: The authors of this article have indicated no relevant relationships that could be perceived as a real or apparent conflict of interest.

CME Credit: SNM is accredited by the Accreditation Council for Continuing Medical Education (ACCME) to sponsor continuing education for physicians. SNM designates each *JNM* continuing education article for a maximum of 1.0 AMA PRA Category 1 Credit. Physicians should claim only credit commensurate with the extent of their participation in the activity.

For CE credit, participants can access this activity through the SNM Web site (http://www.snm.org/ce_online) through January 2012.

Prostate cancer is biologically and clinically a heterogeneous disease that makes imaging evaluation challenging. The role of imaging in prostate cancer should include diagnosis, localization, and characterization (indolent vs. lethal) of the primary tumor, determination of extracapsular spread, guidance and evaluation of local therapy in organ-confined disease, staging of locoregional lymph nodes, detection of locally recurrent and metastatic disease in biochemical relapse, planning of radiation treatment, prediction and assessment of tumor response to salvage and systemic therapy, monitoring of active surveillance and definition of a trigger for definitive therapy, and prognostication of time to hormone refractoriness in castrate disease and overall survival. To address these tasks effectively, imaging needs to be tailored to the specific phases of the disease in a patient-specific, risk-adjusted manner. In this article, I review the preclinical and clinical evidence on the potential and emerging role of PET with the 3 most commonly studied radiotracers in prostate cancer, namely ^{18}F-FDG, ^{18}F- or ^{11}C-acetate, and ^{18}F- or ^{11}C-choline.

Key Words: genitourinary; molecular imaging; PET; PET/CT; acetate; choline; FDG; prostate

J Nucl Med 2011; 52:81–89
DOI: 10.2967/jnumed.110.077941

Among men in the United States, prostate cancer is the second most common cancer (exceeded only by nonmelanoma skin cancers) and the second leading cause of cancer death (exceeded only by lung cancer). In 2009, the incidence of and deaths from this disease were 192,280 cases and 27,360 cases, respectively (*1*). As life expectancy increases, so will the incidence of this disease, creating what will become an epidemic male health problem. Prostate cancer is clinically a heterogeneous disease characterized by an overall long natural history in comparison to the other solid tumors, with a wide spectrum of biologic behavior that ranges from indolent to aggressive (*2*).

Prostate-specific antigen (PSA) screening has resulted in increased detection of clinically insignificant prostate cancers through repeated standard and occasionally saturation biopsies (overdiagnosis and stage migration), which have inevitably led to early unnecessary therapy in many patients (overtreatment). In the post-PSA era, at the time of initial presentation, 80% of patients present with local disease, 12% with regional disease, and 4% with metastatic disease, with the remaining 4% classified as unknown (*1*).

Despite highly successful treatments for localized prostate cancer, approximately 15%–40% of men will experience a detectable rise in the serum PSA level (biochemical failure) within 10 y from the primary treatment, suggesting that prostate cancer can metastasize relatively early in the course of the disease, probably as a result of genetic instability, including loss of metastasis-suppressor genes (*3*). About 25%–35% of men with an increasing serum PSA level will develop locally recurrent disease only, 20%–25% will develop metastatic disease only, and 45%–55% will develop both local recurrence and metastatic disease (*1*). Pound et al., in their landmark article, documented the natural history of progression to metastatic disease and death after PSA elevation after radical prostatectomy and no adjuvant hormonal therapy (*4*). A detectable serum PSA level of at least 0.2 ng/mL was considered evidence of biochemical recurrence. The actuarial metastasis-free survival for all men was 82% at 15 y after surgery. The median

Received Jul. 3, 2010; revision accepted Nov. 18, 2010.
For correspondence or reprints contact: Hossein Jadvar, Keck School of Medicine, University of Southern California, 2250 Alcazar St., CSC 102, Los Angeles, CA 90033.
E-mail: jadvar@usc.edu

actuarial time to metastases was 8 y from the time of PSA relapse. Once men developed metastatic disease, the median survival time to death was 5 y. The time to biochemical progression, PSA doubling time, and Gleason score were predictive of the probability and time to the development of metastatic disease. The interval from surgery to the appearance of metastatic disease was predictive of time until death. Once men develop castrate-resistant metastatic disease, the 1-y survival is about 24%, with a median survival of only 8–18 mo (*4*). The hormone-refractory state is believed to occur via bypassing or sensitizing the androgen receptor signaling pathway. The factors involved may be androgen receptor mutation such that the receptor either is activated promiscuously by different steroids or is activated in a ligand-independent manner. Other factors include amplification of coactivators, activation of oncogenes, and autocrine growth factor stimulation (*5*).

Diagnostic Imaging Evaluation of Prostate Cancer

Imaging evaluation of prostate cancer remains challenging (*6*). The overall role of imaging in prostate cancer should include diagnosis, localization and characterization (indolent vs. lethal) of the primary tumor, determination of extracapsular spread, guidance and evaluation of local therapy in organ-confined disease, staging of locoregional lymph nodes, detection of locally recurrent and metastatic disease in biochemical relapse, planning of radiation treatment, prediction and assessment of tumor response to salvage and systemic therapy, monitoring of active surveillance and definition of a trigger for definitive therapy, and prognostication of time to hormone refractoriness in castrate disease and overall survival.

Initial imaging diagnosis may be made with ultrasound or MRI using endorectal probes and image-guided biopsies when disease is suspected on the basis of a high serum PSA level or abnormal findings on digital rectal examination. Because prostate cancer is often multifocal, and standard 10- to 12-core biopsy may miss 38% of cancers or underrepresent higher-grade tumor foci (which probably drive the overall cancer biologic behavior and outcome), the important role of imaging in localization and characterization of primary tumors becomes clear (*7*). Accurate depiction of the primary tumor foci may guide and evaluate the response to focal therapies ("male lumpectomy") of aggressive cancers (~15% of tumors) and avoid early treatment of indolent cancers, which can then be followed by active surveillance (*8*).

Imaging also provides important information on the local extent of disease and examines for potential regional and distant metastatic disease in high-risk patients. The optimal method for imaging evaluation of men with PSA relapse (biochemical failure) has not been determined, but the goal of imaging is to determine whether there is recurrence in the treated prostate bed or whether distant disease is present (or both), because such a determination affects therapeutic management, including consideration for salvage therapy for local recurrence and systemic treatment for metastatic disease. Despite their overall utility, current imaging tests, including ultrasound, CT, MRI, ^{99m}Tc-based bone scintigraphy, and ^{111}In-capromab pendetide scintigraphy, are not sufficiently accurate in detecting and characterizing disease in prostate cancer (*9*).

In this article, I review the use of the 3 most studied PET radiotracers in prostate cancer: ^{18}F-FDG, ^{18}F- or ^{11}C-labeled acetate, and ^{18}F- or ^{11}C-labeled choline. The discussion is organized by radiotracer, allowing the reader to focus on the information for a particular radiotracer of interest independently of the discussion of other radiotracers. Nested within each radiotracer category is an attempt to present the available information on the basis of disease phases or imaging tasks. However, many studies used patients with a mixture of clinical phases, and hence clear separation of patient categories was often challenging. Moreover, the data on ^{11}C and ^{18}F labels of acetate and choline are presented separately for 2 reasons: first, there are substantially more published data on the ^{11}C labels, and second, it would be helpful to review the ^{18}F label information separately because the pertinent data are rapidly expanding, with results that may differ from those of the ^{11}C label, as does the overall relevance to the clinical setting in view of the longer half-life (110 min) and potential supply availability through regional distribution centers (similar to ^{18}F-FDG). I first briefly review the biologic basis of the relevant radiotracer uptake in prostate tumor and then present the available clinical evidence.

^{18}F-FDG and Prostate Cancer

Molecular Biology Correlates of Tumor Uptake. The ability of ^{18}F-FDG PET to detect cancer is based on elevated glucose metabolism in the malignant tissue in comparison to the normal tissue (Warburg effect) as a result of increased expression of cellular membrane glucose transporters (mainly transporter 1) and enhanced hexokinase II enzymatic activity in tumors (*10,11*).

Few studies have reported on expression of glucose transporters in human prostate cancer. In 1 investigation, the glucose transporter 1 messenger RNA expression was assessed by Northern blot analysis in the androgen-independent cell lines DU145 and PC3 and the androgen-sensitive LNCaP prostate cancer cell line (*12*). Although glucose transporter 1 expression was detected in all 3 cell lines, the level of expression was higher in the poorly differentiated cell lines DU145 and PC3 than in the well-differentiated hormone-sensitive LNCaP cell line, suggesting that the level of glucose transporter 1 expression increases with progression of malignancy grade. Recently, British investigators evaluated the expression of several hypoxia-associated genes within benign prostatic hyperplasia and prostate cancer (Gleason score 5–10) human tissue specimens (*13*). *GLUT1* gene expression was significantly higher in prostate cancer than in benign prostatic hyperplasia and correlated directly with Gleason score (R = 0.274, P =

0.026). These findings may explain not only the observation of higher ^{18}F-FDG accumulation in castration-resistant (androgen-independent) tumors than in castration-sensitive tumors but also the modulatory effect of androgen on the glucose metabolism of castration-sensitive tumors (*14*).

Normal Prostate Tissue. The glucose metabolism and CT density of the normal prostate gland in relation to age and prostate size have been assessed using ^{18}F-FDG PET/CT in 145 men who had indications unrelated to prostate pathology (*15*). The average prostate size was 4.3 ± 0.5 cm (mean ± SD), with a range of 2.9–5.5 cm. Mean and maximum CT densities, in Hounsfield units, were 36.0 ± 5.1 (range, 23–57) and 91.7 ± 20.1 (range, 62–211), respectively, whereas mean and maximum standardized uptake values (SUVs) were 1.3 ± 0.4 (range, 0.1–2.7) and 1.6 ± 0.4 (range, 1.1–3.7), respectively. The mean SUV tended to decrease as the prostate size increased ($r = -0.16$, $P = 0.058$), whereas the prostate size tended to increase with increasing age ($r = 0.32$, $P < 0.001$).

Primary Tumor and Staging. Initial analysis of the data of the National Oncologic PET Registry clearly indicates that ^{18}F-FDG PET can influence the clinical management of men with prostate cancer (from nontreatment to treatment in 25.3% of cases and from treatment to nontreatment in 9.7% of cases), although the influence is lower than for other cancers (*16*). Nevertheless, the overall clinical experience with ^{18}F-FDG PET in prostate cancer suffers from heterogeneity in published studies with regard to the clinical phases of disease, relatively small numbers of patients, and variability and limitations in the validation criteria.

The level of ^{18}F-FDG accumulation can overlap in normal prostate tissue, benign prostatic hyperplasia, and prostate cancer tissues, all of which often coexist (*17*). ^{18}F-FDG PET might not be useful in the diagnosis or staging of clinically organ-confined disease or in the detection of locally recurrent disease because of the relatively similar uptake of ^{18}F-FDG by the posttherapy changes and tumor cells and because of the high level of excreted radiotracer in the adjacent urinary bladder that may mask any lesions in the vicinity (*18*). False-positive results may occur with prostatitis (*19*). Despite the drawbacks and the overall heterogeneity of published studies with relatively small numbers of subjects, several animal-based translational and human-based clinical studies have demonstrated that ^{18}F-FDG PET can be useful in certain clinical circumstances in prostate cancer. ^{18}F-FDG uptake is higher in poorly differentiated primary tumors (Gleason sum score > 7) and higher PSA values than in tumors with lower Gleason scores, a more localized clinical stage, and lower serum PSA values (Fig. 1) (*20*).

^{18}F-FDG PET was less sensitive than ^{99m}Tc-based bone scintigraphy at identifying bone metastases, and detection of pelvic lymph node metastases was limited because of bladder urine activity (*21*). In patients with known osseous metastatic disease, however, ^{18}F-FDG PET might distinguish the metabolically active lesions from the metabolically dormant lesions (*22*). Furthermore, data from our laboratory suggest that the rate of concordance of ^{18}F-FDG PET with other imaging studies may depend on the phase of disease (castrate-resistant vs. castrate-sensitive), time of imaging in relation to therapy (before or during), and type of lesions (lymph node and visceral vs. osseous) (*23*).

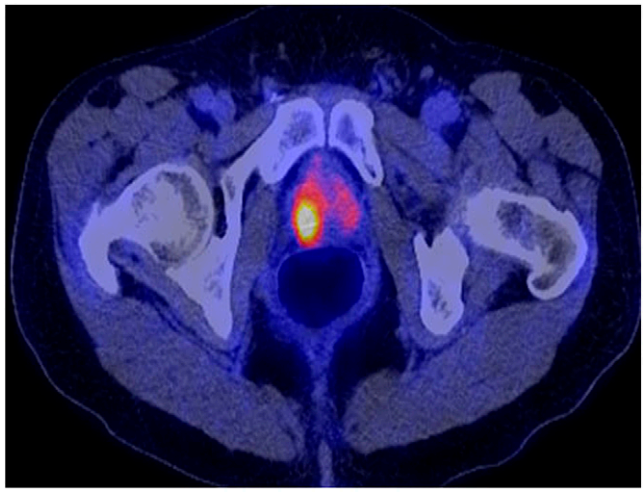

FIGURE 1. A 67-y-old man with biopsy-confirmed prostate cancer (Gleason score, 8; PSA level, 14.6 ng/mL). ^{18}F-FDG PET/CT shows intense hypermetabolism (maximum SUV, 7.7) in right prostate lobe.

Biochemical Failure and Restaging. ^{18}F-FDG PET may be useful in detecting disease in a fraction of the large proportion of men who present with PSA relapse, in whom, by definition, there is no standard imaging evidence of disease. In this group of men, detection of disease by nonstandard imaging can direct appropriate treatment, such as salvage radiation therapy for local recurrence in the prostate bed or systemic therapy for metastatic disease. In a study of 24 patients who had rising serum PSA levels after treatment for localized prostate tumors, ^{18}F-FDG PET was performed before pelvic lymph nodes were dissected (*24*). In none of the patients did pelvic CT yield positive findings. The histology of the pelvic lymph nodes obtained from surgery confirmed the presence of metastases in 67% of patients. Increased ^{18}F-FDG uptake was shown at the sites of histopathologically proven metastases in 75% of these patients. The sensitivity, specificity, accuracy, positive predictive value, and negative predictive value of ^{18}F-FDG PET in detecting metastatic pelvic lymph nodes were 75.0%, 100%, 83.3%, 100%, and 67.7%, respectively. In a similar retrospective study of 91 patients with PSA relapse after prostatectomy and validation of tumor presence by biopsy or clinical and imaging follow-up, mean serum PSA levels were higher in ^{18}F-FDG PET–positive patients than in ^{18}F-FDG PET–negative patients (9.5 ± 2.2 ng/mL vs. 2.1 ± 3.3 ng/mL) (*25*). A PSA level of 2.4 ng/mL and PSA velocity of 1.3 ng/mL/y provided the best compromise between sensitivity (80% for ^{18}F-FDG PET–positive and 71% for ^{18}F-FDG PET–negative patients) and specificity (73% for ^{18}F-FDG PET–positive and 77% for ^{18}F-FDG PET–negative patients) in a receiver-operating-

characteristic curve analysis. Overall, ^{18}F-FDG PET detected local or systemic disease in 31% of patients with PSA relapse. However, confidence in the accuracy and relevance of this figure is somewhat limited in view of the heterogeneity and limitation of the validation criteria—an issue with other similar studies. ^{18}F-FDG PET may also be particularly useful in staging of advanced prostate cancer in patients who have a rising PSA level despite treatment (*26*). Moreover, in this clinical setting, ^{18}F-FDG PET is advantageous over ^{111}In-capromab pendetide scintigraphy in the detection of metastatic disease in patients with high PSA levels or high PSA velocity (*27*).

Therapy Response Assessment. In 1 report, ^{18}F-FDG accumulation in the primary prostate cancer and metastatic sites decreased over a period of 1–5 mo after initiation of androgen deprivation therapy, as was consistent with results from animal xenograft studies (*28*). However, an earlier study of prostate cancer in rats showed that the global ^{18}F-FDG SUV was unchanged after treatment with gemcitabine (*29*). Our preliminary results show that tumor ^{18}F-FDG uptake decreases with successful treatment (using androgen deprivation or various chemotherapy regimens), in general concordance with other measures of response, such as a decline in serum PSA level (Fig. 2) (*30*).

Prognostication. The level and extent of ^{18}F-FDG accumulation in metastatic lesions may provide information on prognosis. An increase of over 33% in the average maximum SUV measurement from up to 5 lesions, or the appearance of new lesions, was reported to be able to categorize castrate-sensitive metastatic prostate cancer patients treated with antimicrotubule chemotherapy into progressors or nonprogressors (*31*). Similarly, another group reported that patients with primary prostate tumors with high SUVs had a poorer prognosis than did those with low SUVs (*32*). Moreover, because ^{18}F-FDG uptake in prostate tumors appears to depend on the presence and activity of androgen, ^{18}F-FDG PET might also be useful in predicting the time to reach the androgen-refractory state (e.g., by an early increase in castrate tumor ^{18}F-FDG uptake), which might facilitate earlier therapeutic modification to avert or delay this clinical state in order to improve overall outcome.

^{18}F- or ^{11}C-Acetate and Prostate Cancer

Molecular Biology Correlates of Tumor Acetate Uptake. Acetate participates in cytoplasmic lipid synthesis, which is believed to be increased in tumors. The cellular retention of radiolabeled acetate in prostate cancer cell lines is primarily due to incorporation of the radiocarbon into phosphatidylcholine and neutral lipids of the cells (*33*). It has been suggested that fatty acid metabolism rather than glycolysis may be dominant in prostate cancer in view of alterations in several enzymes involved in the metabolism of fatty acids and an enhanced β-oxidation pathway (*34*). Recent in vitro and animal model in vivo studies by the group at Washington University in St. Louis confirmed the extensive involvement of the fatty acid synthesis pathway in ^{11}C-acetate uptake in prostate tumors as an imaging marker for fatty acid synthase expression (*35*). Fatty acid synthase is the major enzyme required for converting carbohydrates to fatty acids, and its upregulation plays a role in tumorigenesis of the prostate in the transgenic adenocarcinoma of the mouse prostate model (*36*).

Primary Tumor and Staging. Normal biodistribution of ^{11}C-acetate demonstrates high accumulation in the pancreas,

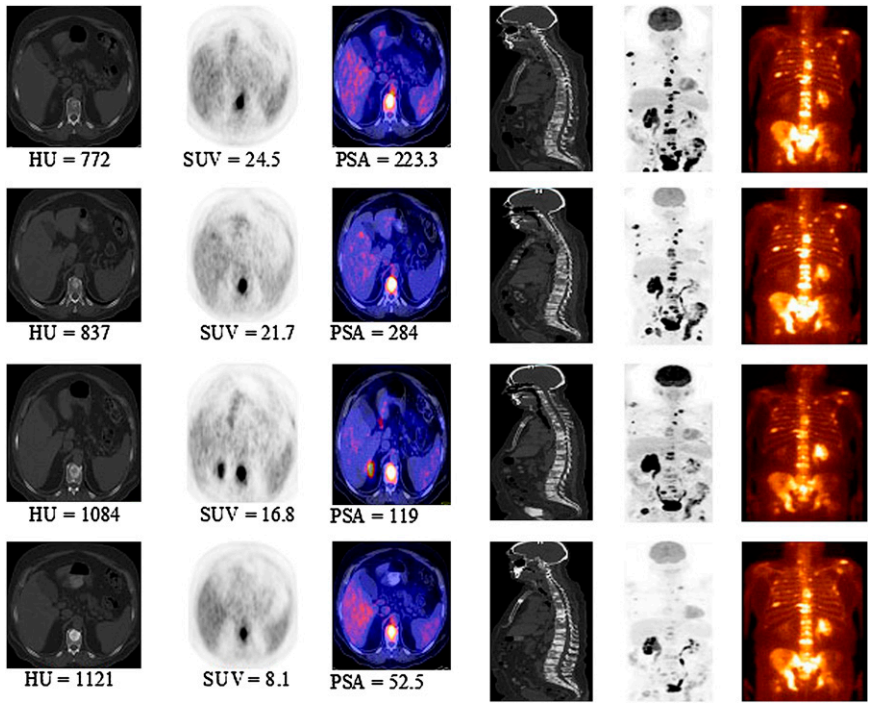

FIGURE 2. Serial ^{18}F-FDG PET/CT and bone scans of 63-y-old man with castrate-resistant metastatic prostate cancer with original primary cancer Gleason score of 9. Rows from top to bottom are scans at baseline (before chemotherapy) and at 4, 8, and 12 mo after initiation of chemotherapy. Columns from left to right are axial CT scans (bone window level), ^{18}F-FDG PET scan, fused PET/CT scans, mid sagittal CT scan (bone window level), PET maximum-intensity-projection images, and ^{99m}Tc-methylene diphosphonate bone scans. Concordant decline in overall metabolic activity of metastatic lesions and PSA level is seen with treatment. Sclerosis of osseous lesions increases as corresponding metabolic activity declines with treatment.

variable uptake in the liver and bowel, and some renal uptake, with little urinary excretion (*37*). The lack of accumulation of ^{11}C-acetate in urine is advantageous to imaging prostate cancer in particular, because the prostate bed remains unobstructed by the adjacent high levels of radioactivity in the urinary bladder, potentially a problem with ^{18}F-FDG. Although there can be a considerable overlap between the uptake level in primary cancer, benign prostatic hyperplasia, and the normal prostate gland, tracer uptake generally appears to be greater in the tumor than in normal and benign prostatic hyperplasia tissue (*38*). Another finding from this study was an age-related physiologic accumulation of ^{11}C-acetate (SUV, 3.4 ± 0.7 in age < 50 y, 2.3 ± 0.7 in age ≥ 50 y). In another study, from Japan, ^{11}C-acetate was compared with ^{18}F-FDG for the detection of primary tumors (*39*). The tumors demonstrated a variable uptake of ^{11}C-acetate (in all 18 patients), with SUVs ranging from 3.3 to 9.9 (measured at 10–20 min after tracer administration), in comparison to ^{18}F-FDG accumulation (in 15/18 patients), which had SUVs ranging from 1.97 to 6.34 (measured at 40–60 min after tracer administration). The authors concluded that ^{11}C-acetate is more sensitive than ^{18}F-FDG in the detection of primary prostate cancer.

Biochemical Failure and Restaging. ^{11}C-acetate may also be useful in the detection of tumor recurrence in some patients who had been treated previously with prostatectomy or radiation, with lesion detectability of 75% and a false-positive rate of up to 15% (Fig. 3) (*40–42*). In a comparative study with ^{18}F-FDG, the median ^{11}C-acetate uptake was higher than ^{18}F-FDG for local recurrence and regional lymph node metastases whereas the reverse was noted with distant metastases (*43*). In another similar study, ^{11}C-acetate identified disease in 30% of patients, in comparison to 9% with ^{18}F-FDG, when analysis was limited to findings confirmed by other correlative imaging studies that were considered to likely represent tumor (*41*). In this same report, the success rate of lesion detection by ^{11}C-acetate was related to serum PSA level, with a 59% positive rate in patients with serum PSA greater than 3 ng/mL that declined significantly to 4% in patients with serum PSA levels of 3 ng/mL or less.

^{18}F-Fluoroacetate. An ^{18}F-labeled formulation of acetate (which allows commercial regional distribution similar to ^{18}F-FDG) has also been reported to have potential use in prostate cancer (*44*). A comparative animal study of ^{11}C-acetate and ^{18}F-fluoroacetate showed that for most organs (except blood, muscle, and fat) the tumor-to-organ uptake ratios at 30 min after tracer administration were higher with ^{18}F-fluoroacetate whereas the tumor-to-heart and tumor-to-prostate ratios were similar (*45*). A recent investigation in Cynomolgus monkeys and pigs showed that ^{18}F-fluoroacetate is not a functional analog of ^{11}C-acetate in normal physiology. ^{18}F-fluoroacetate demonstrated prolonged blood retention, rapid clearance from liver, excretion in bile and urine, and defluorination in pigs (high bone uptake) (*46*).

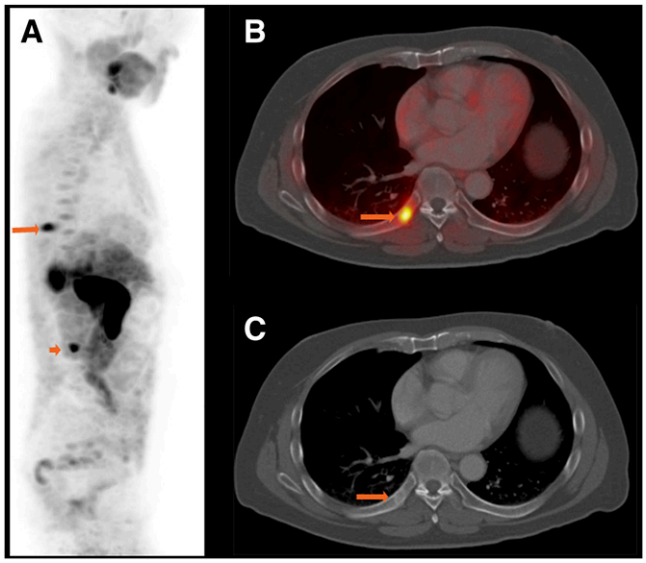

FIGURE 3. A 67-y-old man with history of prostate cancer who had undergone resection and had rising PSA level. ^{11}C-acetate–avid right eighth rib metastasis is seen on maximum-intensity projection (A, long arrow) and selected axial fused (B, arrow) and CT (C, arrow) images, with sclerotic changes seen on CT. Additional L4 vertebral metastasis is seen on maximum-intensity-projection image (A, short arrow). (Courtesy of Martin Allen-Auerbach and Johannes Czernin, University of California, Los Angeles.)

^{18}F- or ^{11}C-Choline and Prostate Cancer

Molecular Biology Correlates of Tumor Choline Uptake. Radiolabeled choline accumulates in prostate tumors (*47*). Therefore, choline PET has been found to be useful in imaging prostate cancer (*48–51*). The biologic basis for radiolabeled choline uptake in tumors is the malignancy-induced upregulation of choline kinase, which leads to the incorporation and trapping of choline in the form of phosphatidylcholine (lecithin) in the tumor cell membrane. Choline uptake in prostate tumors appears not to be correlated with cellular proliferation (as depicted by Ki-67) but may be affected by hypoxia (*52,53*). Under aerobic conditions, both androgen-sensitive and androgen-independent prostate tumors have shown higher choline uptake than that with radiolabeled acetate or with ^{18}F-FDG. However, during hypoxia, the tumor uptake with ^{18}F-FDG and acetate is higher than that with choline (*52*). Both ^{11}C- and ^{18}F-labeled choline have been synthesized and investigated (*54,55*). ^{11}C-choline has a shorter half-life (20 min) that requires an onsite cyclotron. Normal biodistribution of ^{11}C-choline demonstrates relatively high accumulation in the pancreas, liver, kidneys, and salivary glands and variable uptake in the bowel, with little urinary excretion.

Primary Tumor and Staging. A retrospective study compared the diagnostic performance of MRI, 3-dimensional MR spectroscopy, combined MRI–MR spectroscopy, and ^{11}C-choline PET/CT for intraprostatic tumor sextant localization, with histology as the standard of reference (*56*). The sensitivity and specificity were 55% and 86%,

respectively, for PET/CT, 54% and 75%, respectively, for MRI, and 81% and 67%, respectively, for MR spectroscopy. Therefore, in this study, ^{11}C-choline PET/CT demonstrated a lower sensitivity relative to MR spectroscopy alone or combined with MRI. Opposite findings have been reported by the Japanese investigators in that ^{11}C-choline PET was more sensitive than MRI and MR spectroscopy for detection of primary prostate lesions (100% for PET vs. 60% for MRI vs. 65% for MR spectroscopy) (*57*). These conflicting results may be due to differing methodology in data collection or analysis and in patient populations. Research is under way to provide more sophisticated image fusion software for accurate registration of anatomic MRI, diffusion MRI, ^{11}C-choline PET, and histologic sections of the prostate gland—fusion that may be facilitated by the emergence of the hybrid PET/MRI systems (*58*).

German investigators compared ^{11}C-choline PET/CT with whole-body MRI retrospectively for staging of prostate cancer (*59*). Diagnostic validation was by histology, follow-up, or consensus reading. Overall sensitivity and specificity were 97% and 77%, respectively, for ^{11}C-choline PET and 79% and 94%, respectively, for whole-body MRI. Therefore the 2 imaging modalities were complementary. A study similar to the MRI reports, comparing transrectal ultrasonography and ^{11}C-choline PET/CT in patients with clinically localized prostate cancer, showed that both PET and transrectal ultrasonography tended to understage prostate cancer. The authors therefore suggested that reliable clinical decision making (e.g., with regard to decisions on nerve-sparing radical prostatectomy) based on the findings on these imaging modalities might not be possible (*60*). Despite these reports, other investigations have found a relatively good diagnostic performance for ^{11}C-choline PET and PET/CT in the detection of primary prostate cancer. For example, Scher et al. reported a sensitivity of 87% and specificity of 62% for the detection primary prostate cancer, with histopathologic examination of resection specimens or biopsy as the reference standard (*61*). Interestingly, the group from Italy reported nearly the reverse values, with sensitivity of 66% and specificity of 81% for localization of primary prostate cancer on a sextant histopathologic analysis (*62*). Martorana et al. assessed the diagnostic performance of ^{11}C-choline PET/CT for nodules 5 mm or larger in 43 patients with known prostate cancer before the initial 12-core transrectal biopsy (*63*). PET demonstrated a sensitivity of 83% in this setting but had lower sensitivity than MRI for the assessment of extraprostatic extension (22% vs. 63%, respectively, $P < 0.001$). Therefore, although ^{11}C-choline PET may be helpful in detecting primary prostate cancer, the sensitivity may depend on several factors that will need to be defined (e.g., tumor grade, size, and location).

Biochemical Failure and Restaging. ^{11}C-choline PET has been evaluated for detecting local, regional, and metastatic prostate cancer (*64*). The tracer uptake was noted to decrease both in the primary tumor and in metastases after hormonal therapy, although this finding has been disputed in other studies (*47,65*). In another study, ^{11}C-choline was determined to localize recurrence in a higher percentage of men after primary radiation therapy than after radical prostatectomy (78% vs. 38%, respectively) (*49*). The reason for such a difference based on the type of primary therapy is unclear. Potential utility for ^{11}C-choline PET/CT in the detection of local recurrence after radical prostatectomy has also been demonstrated with a sensitivity of 73% and specificity of 88% (*51*). The Italian researchers reported a sensitivity and specificity of 64% and 90%, respectively, for the detection of nodal metastases in men with PSA failure after radical retropubic prostatectomy (*66*).

A positive correlation between ^{11}C-choline PET/CT lesion detection rate and PSA level has been reported, although there are also reports of no significant correlation (patient-based analysis) between lesion maximum SUV, PSA level, Gleason score, and pathologic stage at the time of initial diagnosis (*67,68*). In the study by Krause et al., from Germany, the detection rate of ^{11}C-choline PET/CT was 36% for PSA < 1 ng/mL, 43% for $1 \leq$ PSA < 2 ng/mL, 62% for $2 \leq$ PSA < 3 ng/mL, and 73% for PSA ≥ 3 ng/mL (*65*). Castellucci et al., from Italy, evaluated the likelihood of lesion detection in 190 men after radical prostatectomy who presented with PSA relapse (defined as PSA > 0.2 ng/mL; range, 0.2–25.4 ng/mL; mean, 4.2 ng/mL) (*69*). The authors found that the likelihood of lesion detection by the nonstandard imaging evaluation with ^{11}C-choline PET was increased when PSA was higher than 2.4 ng/mL or when PSA was less than 2.4 ng/mL but that the PSA doubling time was lower than 3.4 mo or PSA velocity was higher than 1 ng/mL/y. However, this study included some patients with abnormal standard imaging evidence of disease that did not satisfy the pure-definition requirement of PSA relapse-only disease with negative standard imaging results.

In a more recent investigation, dual-tracer ^{11}C-choline and ^{18}F-FDG PET were investigated in detecting disease in 73 men with PSA relapse after radical prostatectomy (67.1% of patients), radiation therapy (32.9% of patients), and adjuvant hormonal therapy (20.5% of patients) (*70*). The PSA range and median were 0.87–5.4 and 2.4 ng/mL, respectively, for the radical prostatectomy group and 2.1–5.57 and 3.5, respectively, for the radiation therapy group. The Gleason score for the primary disease was 2–7 (well to moderately differentiated) in 69.9% of patients and 8–10 (poorly differentiated) for 27.4% of patients. The standard of reference was biopsy, increase in PSA without therapy, and decrease in PSA after therapy. The authors reported a sensitivity of 60.6% for ^{11}C-choline and 31% for ^{18}F-FDG at all PSA levels. Additionally they noted that ^{18}F-FDG correlated better with Gleason score than did ^{11}C-choline. They concluded that although ^{11}C-choline appears to be more sensitive than ^{18}F-FDG for the detection of disease in PSA relapse, ^{18}F-FDG was better in discriminating the proliferative character of the disease.

In summary, despite some mixed results, it appears that the sensitivity of PET may generally depend directly on

serum PSA level, with the expectation that at higher PSA levels, the probability of lesion localization increases. Moreover, ^{11}C-acetate and ^{11}C-choline appear to be about equally useful in imaging prostate cancer in individual patients (*71*).

^{18}F-Fluorocholine. An ^{18}F-labeled formulation of choline has also been developed and preliminarily tested in men with prostate cancer (Fig. 4). Price et al. showed that murine xenografts of prostate cancer accumulated higher ^{18}F-FDG than ^{18}F-fluorocholine whereas, interestingly, in humans the ^{18}F-fluorocholine uptake in lesions was higher than the ^{18}F-FDG uptake (*72*). The exact reason for such an observation is unclear but may be due to the biologic differences between an implanted tumor and a native tumor. A recent animal study from our group showed that uptake interval and castration do not significantly affect the level of choline uptake in prostate tumors (*47*).

The normal biodistribution of ^{18}F-fluorocholine demonstrates relatively high accumulation in the pancreas, liver, spleen, and kidneys; variable uptake in the bowel; and excretion into urine. ^{18}F-fluorocholine uptake overlaps among normal, benign, and malignant prostate tissues (similar to ^{11}C-acetate and ^{11}C-choline) (*73*). In a recent report, disease was missed in a significant number of patients ($\leq$75%) with elevated PSA (*73*), although in another report the results were more encouraging (*74*).

Beheshti et al. examined the potential utility of ^{18}F-fluorocholine PET/CT in men who had clinical organ-confined tumor but were at intermediate (PSA = 10–20 ng/mL, Gleason score = 7) and high (PSA > 20 ng/mL, Gleason score $\geq$ 8) risk for extracapsular extension before undergoing radical prostatectomy with extended pelvic lymph node dissection (*75*). The sensitivity, specificity, positive predictive value, and negative predictive value of ^{18}F-fluorocholine for detection of pelvic lymphadenopathy were 45%, 96%, 82%, and 83% for all lymph node sizes, respectively, and 66%, 96%, 82%, and 92% for those lymph nodes greater than or equal to 5 mm. Not surprisingly, the diagnostic performance improved when nodes smaller than the PET spatial resolution were excluded.

Another study from the same group of investigators correlated the uptake of ^{18}F-fluorocholine in bone metastases with the morphologic changes on CT in 70 men with prostate cancer (*76*). The standard of reference was other imaging and clinical follow-up. The overall sensitivity and specificity of ^{18}F-fluorocholine for the detection of bone metastases were 79% and 97%, respectively. Lytic lesions demonstrated higher metabolism than blastic lesions (average maximum SUV of 11 $\pm$ 3.2 for lytic lesions vs. 7.8 $\pm$ 3.0 for blastic lesions). No statistically significant difference was found in the maximum SUV of lesions in relation to the presence or absence of hormonal therapy. Conversely, the bone lesion CT density was significantly higher in patients receiving hormonal therapy. The authors identified 3 correlative PET/CT patterns for bone metastases: lesions with ^{18}F-fluorocholine uptake only, probably representing bone marrow infiltration without morphologic changes on CT; lesions with both ^{18}F-fluorocholine uptake and CT morphologic changes; and lesions with no ^{18}F-fluorocholine uptake but displaying dense sclerosis on CT (Hounsfield units > 825), probably indicating nonviable tumor. We have observed similar findings with ^{18}F-FDG PET/CT in bone metastases of prostate cancer (*23*). The same group of researchers also compared ^{18}F-fluorocholine and ^{18}F-fluoride PET/CT in the detection of bone metastases (*77*). This study revealed that ^{18}F-fluorocholine might be superior for early detection (i.e., bone marrow involvement) of metastatic bone disease and that in patients with ^{18}F-fluorocholine–negative suggestive sclerotic lesions, ^{18}F-fluoride can be helpful, with the caveat that ^{18}F-fluoride PET could also be negative in highly dense sclerotic lesions, presumably reflecting treated disease. Therefore, metabolic and morphologic changes of bone metastases are dynamic processes, and combined imaging is best suited to capture the natural course of these changes to allow for management decisions and accurate assessment of treatment response.

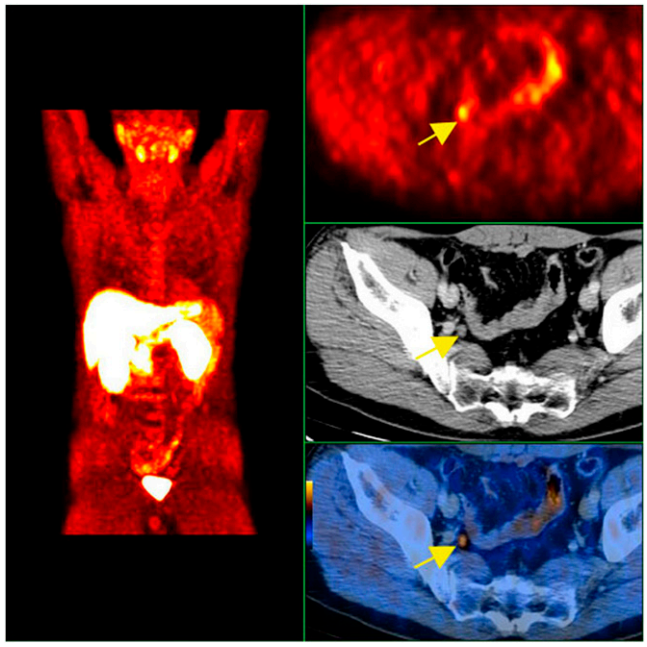

FIGURE 4. A 60-y-old man with history of prostate cancer who had undergone resection and had rising PSA level. Right column from top to bottom shows ^{18}F-fluorocholine PET, pelvis CT, and fused PET/CT images demonstrating abnormal accumulation of radiotracer in normal-sized right internal iliac lymph node (arrows). Maximum-intensity-projection image on left shows normal biodistribution of ^{18}F-fluorocholine and no other suggestive lesions. (Courtesy of Mohsen Beheshti, St. Vincent's Hospital, Linz, Austria.)

In relation to men with biochemical failure, the Italian investigators showed that the detection rate of ^{18}F-fluorocholine PET/CT in patients with biochemical relapse positively correlates with the serum PSA level, similarly to the results of ^{11}C-choline studies (*78*). In this study, ^{18}F-fluorocholine PET demonstrated a detection rate of 20% for PSA $\leq$ 1 ng/mL, 44% for 1 < PSA $\leq$ 5 ng/mL, and

82% for PSA > 5 ng/mL. Another study, from Austria, demonstrated a 41% true-positive rate in restaging patients with a PSA level of less than 5 ng/mL (*79*). Thus, the decision to use, and expectation of outcome for, ^{18}F-fluorocholine (or ^{11}C-choline) PET in an individual patient with PSA relapse may be adapted to the relevant PSA level (and probably other PSA-derived parameters) (*80*).

SUMMARY

Biologically and clinically, prostate cancer is a heterogeneous disease that is characterized by states ranging from indolent to aggressive. The use of PET in prostate cancer should be considered in the context of the limitations and challenges associated with other imaging modalities in prostate cancer.

Current evidence indicates that ^{18}F-FDG PET might be useful in diagnosis and staging of primary tumors that are known or suspected to have a high Gleason score, in detection of metastatic disease in a fraction of men with biochemical failure with scan sensitivity that increases with increasing PSA level, in assessment of the extent of metabolically active castrate-resistant disease, in monitoring response to androgen deprivation and other therapies, and in prognostication. ^{18}F-FDG PET has limited use in the diagnosis and staging of clinically organ-confined disease and can give false-negative results because of the uptake of ^{18}F-FDG by normal tissue, benign prostatic hyperplasia, and posttherapy changes, as well as false-positive results in the setting of inflammation and infection.

Both ^{11}C-acetate and ^{11}C-choline appear to be somewhat equally useful in imaging prostate cancer in individual patients, although more comparative data are needed. ^{11}C-choline and, more recently, ^{18}F-fluorocholine are increasingly used in many centers in Europe and Japan for the detection of locally recurrent or metastatic disease in men with biochemical failure, with scan sensitivity that correlates positively with serum PSA level. Like ^{18}F-FDG, choline and acetate cannot differentiate between malignant and benign prostate disease. ^{11}C-choline PET may be helpful in detecting primary prostate cancer, but the sensitivity may depend on several factors that will need to be defined (e.g., PSA level, tumor grade, size, and location). There are also mixed findings about the effect of androgen deprivation therapy on choline uptake in prostate tumors, probably due to the heterogeneity of androgen receptor function.

It is clear that prospective clinical imaging trials using various PET tracers, singly or in combination, in different clinical-state–specific patient cohorts with well-defined endpoints, will be needed to decipher the optimal use of PET in prostate cancer.

ACKNOWLEDGMENT

This work was supported by National Institutes of Health–National Cancer Institute grants R01-CA111613 and R21-CA142426.

REFERENCES

1. SEER Stat Fact Sheets: Prostate. Available at: http://seer.cancer.gov/statfacts/html/prost.html. Accessed November 19, 2010.
2. Kessler B, Albertsen P. The natural history of prostate cancer. *Urol Clin North Am.* 2003;30:219–226.
3. Dong JT, Rinker-Schaeffer CW, Ichikawa T, et al. Prostate cancer: biology of metastasis and its clinical implications. *World J Urol.* 1996;14:182–189.
4. Pound CR, Partin AW, Eisenberger MA, et al. Natural history of progression after PSA elevation following radical prostatectomy. *JAMA.* 1999;281:1591–1597.
5. Jenster G. The role of the androgen receptor in the development and progression of prostate cancer. *Semin Oncol.* 1999;26:407–421.
6. Jadvar H, Alavi A. Role of imaging in prostate cancer. *PET Clin.* 2009;4:135–138.
7. Patel AR, Jones JS, Rabets J, et al. Parasagittal biopsies add minimal information in repeat saturation prostate biopsy. *Urology.* 2004;63:87–89.
8. Mazzucchelli R, Scarpelli M, Cheng L, et al. Pathology of prostate cancer and focal therapy ('male lumpectomy'). *Anticancer Res.* 2009;29:5155–5161.
9. Engelbrecht MR, Barentsz JO, Jager GJ, et al. Prostate cancer staging with imaging. *BJU Int.* 2000;86(suppl 1):123–134.
10. Macheda ML, Rogers S, Bets JD. Molecular and cellular regulation of glucose transport (GLUT) proteins in cancer. *J Cell Physiol.* 2005;202:654–662.
11. Smith TA. Mammalian hexokinases and their abnormal expression in cancer. *Br J Biomed Sci.* 2000;57:170–178.
12. Effert P, Beniers AJ, Tamimi Y, et al. Expression of glucose transporter 1 (GLUT-1) in cell lines and clinical specimen from human prostate adenocarcinoma. *Anticancer Res.* 2004;24:3057–3063.
13. Stewart GD, Gray K, Pennington CJ, et al. Analysis of hypoxia-associated gene expression in prostate cancer: lysyl oxidase and glucose transporter 1 expression correlate with Gleason score. *Oncol Rep.* 2008;20:1561–1567.
14. Jadvar H, Li X, Shahinian A, et al. Glucose metabolism of human prostate cancer mouse xenografts. *Mol Imaging.* 2005;4:91–97.
15. Jadvar H, Ye W, Groshen S, et al. [F-18]-fluorodeoxyglucose PET–CT of the normal prostate gland. *Ann Nucl Med.* 2008;22:787–793.
16. Hillner BE, Siegel BA Shields AF, et al. relationship between cancer type and impact of PET and PET/CT on intended management: findings of the National Oncologic PET registry. *J Nucl Med.* 2008;49:1928–1935.
17. Salminen E, Hogg A, Binns D, et al. Investigations with FDG PET scanning in prostate cancer show limited value for clinical practice. *Acta Oncol.* 2002;41:425–429.
18. Liu IJ, Zafar MB, Lai YH, et al. Fluorodeoxyglucose positron emission tomography studies in diagnosis and staging of clinically organ-confined prostate cancer. *Urology.* 2001;57:108–111.
19. Kao PF, Chou YH, Lai CW. Diffuse FDG uptake in acute prostatitis. *Clin Nucl Med.* 2008;33:308–310.
20. Oyama N, Akino H, Suzuki Y, et al. The increased accumulation of [^{18}F]fluorodeoxyglucose in untreated prostate cancer. *Jpn J Clin Oncol.* 1999;29:623–629.
21. Shreve PD, Grossman HB, Gross MD, et al. Metastatic prostate cancer: initial findings of PET with FDG. *Radiology.* 1996;199:751–756.
22. Morris MJ, Akhurst T, Osman I, et al. Fluorinated deoxyglucose positron emission tomography imaging in progressive metastatic prostate cancer. *Urology.* 2002;59:913–918.
23. Jadvar H, Pinski J, Quinn D, et al. PET/CT with FDG in metastatic prostate cancer: castrate-sensitive vs. castrate-resistant disease [abstract]. *J Nucl Med.* 2009;50(suppl):120P.
24. Chang CH, Wu HC, Tsai JJ, et al. Detecting metastatic pelvic lymph nodes by ^{18}F-2-deoxyglucose positron emission tomography in patients with prostate-specific antigen relapse after treatment for localized prostate cancer. *Urol Int.* 2003;70:311–315.
25. Schoder H, Herrmann K, Gonen M, et al. 2-[^{18}F]fluoro-2-deoxyglucose positron emission tomography for detection of disease in patients with prostate-specific antigen relapse after radical prostatectomy. *Clin Cancer Res.* 2005;11:4761–4769.
26. Sung J, Espiritu JI, Segall GM, et al. Fluorodeoxyglucose positron emission tomography studies in the diagnosis and staging of clinically advanced prostate cancer. *BJU Int.* 2003;92:24–27.
27. Seltzer MA, Barbaric Z, Belldegrun A, et al. Comparison of helical computerized tomography, positron emission tomography and monoclonal antibody scans for evaluation of lymph node metastases in patients with prostate specific antigen relapse after treatment for localized prostate cancer. *J Urol.* 1999;162:1322–1328.
28. Oyama N, Akino H, Suzuki Y, et al. FDG PET for evaluating the change of glucose metabolism in prostate cancer after androgen ablation. *Nucl Med Commun.* 2001;22:963–969.

29. Haberkorn U, Bellemann ME, Altmann A, et al. PET 2-fluoro-2-deoxyglucose uptake in rat prostate adenocarcinoma during chemotherapy with gemcitabine. *J Nucl Med.* 1997;38:1215–1221.
30. Jadvar H. Molecular imaging of prostate cancer with ^{18}F-fluorodeoxyglucose PET. *Nat Rev Urol.* 2009;6:317–323.
31. Morris MJ, Akhurst T, Larson SM, et al. Fluorodeoxyglucose positron emission tomography as an outcome measure for castrate metastatic prostate cancer treated with antimicrotubule chemotherapy. *Clin Cancer Res.* 2005;11:3210–3216.
32. Oyama N, Akino H, Suzuki Y, et al. Prognostic value of 2-deoxy-2-[F-18]fluoro-D-glucose positron emission tomography imaging for patients with prostate cancer. *Mol Imaging Biol.* 2002;4:99–104.
33. Yoshimoto M, Waki A, Yonekura Y, et al. Characterization of acetate metabolism in tumor cells in relation to cell proliferation: acetate metabolism in tumor cells. *Nucl Med Biol.* 2001;28:117–122.
34. Liu Y. Fatty acid oxidation is a dominant bioenergetic pathway in prostate cancer. *Prostate Cancer Prostatic Dis.* 2006;9:230–234.
35. Vavere AL, Kridel SJ, Wheeler FB, et al. 1-^{11}C-acetate as a PET radiopharmaceutical for imaging fatty acid synthase expression in prostate cancer. *J Nucl Med.* 2008;49:327–334.
36. Pflug BR, Pecher SM, Brink AW, et al. Increased fatty acid synthase expression and activity during progression of prostate cancer in the TRAMP model. *Prostate.* 2003;57:245–254.
37. Seltzer MA, Jahan SA, Sparks R, et al. Radiation dose estimates in humans for ^{11}C-acetate whole-body PET. *J Nucl Med.* 2004;45:1233–1236.
38. Kato T, Tsukamoto E, Kuge Y, et al. Accumulation of [^{11}C]acetate in normal prostate and benign prostatic hyperplasia: comparison with prostate cancer. *Eur J Nucl Med Mol Imaging.* 2002;29:1492–1495.
39. Oyama N, Akino H, Kanamaru H, et al. ^{11}C-acetate PET imaging of prostate cancer. *J Nucl Med.* 2002;43:181–186.
40. Kotzerke J, Volkmer BG, Neumaier B, et al. Carbon-11 acetate positron emission tomography can detect local recurrence of prostate cancer. *Eur J Nucl Med Mol Imaging.* 2002;29:1380–1384.
41. Oyama N, Miller TR, Dehdashti F, et al. ^{11}C-acetate PET imaging of prostate cancer: detection of recurrent disease at PSA relapse. *J Nucl Med.* 2003;44:549–555.
42. Sandblom G, Sorensen J, Lundin N, et al. Positron emission tomography with ^{11}C-acetate for tumor detection and localization in patients with prostate specific antigen relapse after radical prostatectomy. *Urology.* 2006;67:996–1000.
43. Fricke E, Machtens S, Hofmann M, et al. Positron emission tomography with ^{11}C-acetate and ^{18}F-FDG in prostate cancer patients. *Eur J Nucl Med Mol Imaging.* 2003;30:607–611.
44. Matthies A, Ezziddin S, Ulrich EM, et al. Imaging of prostate cancer metastases with ^{18}F-fluoroacetate using PET/CT. *Eur J Nucl Med Mol Imaging.* 2004;31:797.
45. Ponde DE, Dence CS, Oyama N, et al. ^{18}F-fluoroacetate: a potential acetate analog for prostate tumors imaging—in vivo evaluation of ^{18}F-fluoroacetate versus ^{11}C-acetate. *J Nucl Med.* 2007;48:420–428.
46. Lindhe O, Sun A, Ulin J, et al. [^{18}F]fluoroacetate is not a functional analogue of [^{11}C]acetate in normal physiology. *Eur J Nucl Med Mol Imaging.* 2009;36:1453–1459.
47. Jadvar H, Gurbuz A, Li X, et al. Choline autoradiography of human prostate cancer xenograft: effect of castration. *Mol Imaging.* 2008;7:147–152.
48. Kotzerke J, Prang J, Neumaier B, et al. Experience with carbon-11 choline positron emission tomography in prostate carcinoma. *Eur J Nucl Med.* 2000;27:1415–1419.
49. de Jong IJ, Pruim J, Elsinga PH, et al. ^{11}C-choline positron emission tomography for the evaluation after treatment of localized prostate cancer. *Eur Urol.* 2003;44:38–38.
50. Reske SN. [^{11}C]choline uptake with PET/CT for the initial diagnosis of prostate cancer: relation to PSA levels, tumor stage and anti-androgenic therapy. *Eur J Nucl Med Mol Imaging.* 2008;35:1740–1741.
51. Reske SN, Blumstein NM, Glatting G. [^{11}C]choline PET/CT imaging in occult local relapse of prostate cancer after radical prostatectomy. *Eur J Nucl Med Mol Imaging.* 2008;35:9–17.
52. Hara T, Bansal A, DeGrado TR. Effect of hypoxia on the uptake of [methyl-^{3}H] choline, [1-^{14}C]acetate and [^{18}F]FDG in cultured prostate cancer cells. *Nucl Med Biol.* 2006;33:977–984.
53. Breeuwsma AJ, Pruim J, Jongen MM, et al. In vivo uptake of [^{11}C]choline does not correlate with cell proliferation in human prostate cancer. *Eur J Nucl Med Mol Imaging.* 2005;32:668–673.
54. Reischl G, Bieg C, Schmiedl O, et al. Highly efficient automated synthesis of [^{11}C]choline for multi dose utilization. *Appl Radiat Isot.* 2004;60:835–838.
55. DeGrado TR, Coleman RE, Wang S, et al. Synthesis and evaluation of ^{18}F-labeled choline as an oncologic tracer for positron emission tomography: initial findings in prostate cancer. *Cancer Res.* 2001;61:110–117.
56. Testa C, Schiavina R, Lodi R, et al. Prostate cancer: sextant localization with MR imaging, MR spectroscopy, and ^{11}C-choline PET-CT. *Radiology.* 2007;244:797–806.
57. Yamaguchi T, Lee J, Uemura H, et al. Prostate cancer: a comparative study of ^{11}C-choline PET and MR imaging combined with proton MR spectroscopy. *Eur J Nucl Med Mol Imaging.* 2005;32:742–748.
58. Park H, Piert MR, Khan A, et al. Registration methodology for histological sections and in vivo imaging of human prostate. *Acad Radiol.* 2008;15:1027–1039.
59. Eschmann SM, Pfannenberg AC, Rieger A, et al. Comparison of ^{11}C-choline PET/CT and whole body-MRI for staging of prostate cancer. *Nuklearmedizin.* 2007;46:161–168.
60. Rinnab L, Blumstein NM, Mottaghy FM, et al. ^{11}C-choline positron emission tomography/computed tomography and transrectal ultrasonography for staging localized prostate cancer. *BJU Int.* 2007;99:1421–1426.
61. Scher B, Seitz M, Albinger W, et al. Value of ^{11}C-choline PET and PET-CT in patients with suspected prostate cancer. *Eur J Nucl Med Mol Imaging.* 2007;34:45–53.
62. Farsad M, Schiavina R, Castellucci P, et al. Detection and localization of prostate cancer: correlation of ^{11}C-choline PET/CT with histopathologic step-section analysis. *J Nucl Med.* 2005;46:1642–1649.
63. Martorana G, Schiavina R, Cort B, et al. ^{11}C-choline positron emission tomography/computed tomography for tumor localization of primary prostate cancer in comparison with 12-core biopsy. *J Urol.* 2006;176:954–960.
64. Picchio M, Crivellaro C, Giovacchini G, et al. PET-CT for treatment planning in prostate cancer. *Q J Nucl Med Mol Imaging.* 2009;53:245–268.
65. Krause BJ, Souvatzpglou M, Tuncel M, et al. The detection rate of [^{11}C]choline-PET/CT depends on the serum PSA-value in patients with biochemical recurrence of prostate cancer. *Eur J Nucl Med Mol Imaging.* 2008;35:18–23.
66. Scattoni V, Picchio M, Suardi N, et al. Detection of lymph-node metastases with integrated [^{11}C]choline PET/CT in patients with PSA failure after radical retropubic prostatectomy: results confirmed by open pelvic-retroperitoneal lymphadenectomy. *Eur Radiol.* 2007;52:423–429.
67. Rinnab L, Mottaghy FM, Blumstein NM, et al. Evaluation of [^{11}C]choline positron emission tomography in patients with increasing prostate-specific antigen levels after primary treatment for prostate cancer. *BJU Int.* 2007;100:786–793.
68. Giovacchini G, Picchio M, Coradesschi E, et al. ^{11}C-choline uptake with PET/CT for the initial diagnosis of prostate cancer: relation to PSA levels, tumor stage and anti-androgenic therapy. *Eur J Nucl Med Mol Imaging.* 2008;35:1065–1073.
69. Castellucci P, Fuccio C, Nanni C, et al. Influence of trigger PSA and PSA kinetics on ^{11}C-choline PET/CT detection rate in patients with biochemical relapse after radical prostatectomy. *J Nucl Med.* 2009;50:1394–1400.
70. Richter JA, Rodríguez M, Rioja J, et al. Dual tracer ^{11}C-choline and FDG-PET in the diagnosis of biochemical prostate cancer relapse after radical treatment. *Mol Imaging Biol.* 2010;12:210–217.
71. Kotzerke J, Volkmer BG, Glatting G, et al. Intraindividual comparison of [^{11}C] acetate and [^{11}C]choline PET for detection of metastases of prostate cancer. *Nuklearmedizin.* 2003;42:25–30.
72. Price DT, Coleman RE, Liao RP, et al. Comparison of [18 F]fluorocholine and [18 F]fluorodeoxyglucose for positron emission tomography of androgen dependent and androgen independent prostate cancer. *J Urol.* 2002;168:273–280.
73. Igerc I, Kohlfurst S, Gallowitsch HJ, et al. The value of ^{18}F-choline PET/CT in patients with elevated PSA-level and negative prostate needle biopsy for localization of prostate cancer. *Eur J Nucl Med Mol Imaging.* 2008;35:976–983.
74. Kwee SA, Coel MN, Lim J, et al. Prostate cancer localization with 18fluorine fluorocholine positron emission tomography. *J Urol.* 2005;173:252–255.
75. Beheshti M, Imamovic L, Broinger G, et al. ^{18}F choline PET/CT in the preoperative staging of prostate cancer in patients with intermediate or high risk of extracapsular disease: a prospective study of 130 patients. *Radiology.* 2010;254:925–933.
76. Beheshti M, Vali R, Waldenberger P, et al. The use of F-18 choline PET in the assessment of bone metastases in prostate cancer: correlation with morphological changes on CT. *Mol Imaging Biol.* 2009;11:446–454.
77. Beheshti M, Vali R, Waldenberger P, et al. Detection of bone metastases in patients with prostate cancer by ^{18}F fluorocholine and ^{18}F fluoride PET-CT: a comparative study. *Eur J Nucl Med Mol Imaging.* 2008;35:1766–1774.
78. Pelosi E, Arena V, Skanjeti A, et al. Role of whole-body (^{18}F)-choline PET/CT in disease detection in patients with biochemical relapse after radical treatment for prostate cancer. *Radiol Med.* 2008;113:895–904.
79. Heinisch M, Dirisamer A, Loidl W, et al. Positron emission tomography/computed tomography with F-18 fluorocholine for restaging of prostate cancer patients: meaningful at PSA $<$ 5 ng/mL? *Mol Imaging Biol.* 2006;8:43–48.
80. Apolo AB, Pandit-Taskar N, Morris MJ. Novel tracers and their development for the imaging of metastatic prostate cancer. *J Nucl Med.* 2008;49:2031–2041.

JNM The Journal of NUCLEAR MEDICINE

Prostate Cancer: PET with ^{18}F-FDG, ^{18}F- or ^{11}C-Acetate, and ^{18}F- or ^{11}C-Choline

Hossein Jadvar

J Nucl Med. 2011;52:81-89.
Published online: December 13, 2010.
Doi: 10.2967/jnumed.110.077941

The Journal of Nuclear Medicine is published monthly.
SNMMI | Society of Nuclear Medicine and Molecular Imaging
1850 Samuel Morse Drive, Reston, VA 20190.
(Print ISSN: 0161-5505, Online ISSN: 2159-662X)

SNMMI SOCIETY OF NUCLEAR MEDICINE AND MOLECULAR IMAGING